AECRL-TR-73-0151
2 MARCH 1973 27p.
AIR FORCE SURVEYS IN GEOPHYSICS, NO. 259

AIR FORCE CAMBRIDGE RESEARCH LABORATORIES
L. G. HANSCOM FIELD, BEDFORD, MASSACHUSETTS

Analog Model 1972 of the Arctic Ionosphere

G.J. GASSMANN

AIR FORCE SYSTEMS COMMAND
United States Air Force

AFCRL-TR-73-0151
2 MARCH 1973
AIR FORCE SURVEYS IN GEOPHYSICS, NO. 259

IONOSPHERIC PHYSICS LABORATORY PROJECT 5631

AIR FORCE CAMBRIDGE RESEARCH LABORATORIES

L. G. HANSCOM FIELD, BEDFORD, MASSACHUSETTS

Analog Model 1972 of the Arctic Ionosphere

G.J. GASSMANN

AIR FORCE SYSTEMS COMMAND
United States Air Force

Unclassified
Security Classification

DOCUMENT CONTROL DATA - R&D

(Security classification of title, body of abstract and indexing annotation must be entered when the overall report is classified)

1. ORIGINATING ACTIVITY *(Corporate author)*
Air Force Cambridge Research Laboratories (LIB)
L. G. Hanscom Field
Bedford, Massachusetts 01730

2a. REPORT SECURITY CLASSIFICATION
Unclassified

2b. GROUP

3. REPORT TITLE

ANALOG MODEL 1972 OF THE ARCTIC IONOSPHERE

4. DESCRIPTIVE NOTES *(Type of report and inclusive dates)*
Scientific. Interim.

5. AUTHOR(S) *(First name, middle initial, last name)*

G. J. Gassmann

6. REPORT DATE	7a. TOTAL NO. OF PAGES	7b. NO. OF REFS
2 March 1973	27	20

8a. CONTRACT OR GRANT NO.	9a. ORIGINATOR'S REPORT NUMBER(S)
b. PROJECT, TASK, WORK UNIT NOS. 5631-14-01	AFCRL-TR-73-0151
c. DOD ELEMENT 61102F	9b. OTHER REPORT NO(S) *(Any other numbers that may be assigned this report)*
d. DOD SUBELEMENT 681310	AFSG, No. 259

10. DISTRIBUTION STATEMENT

Approved for public release; distribution unlimited.

11. SUPPLEMENTARY NOTES	12. SPONSORING MILITARY ACTIVITY
TECH, OTHER	Air Force Cambridge Research Laboratories (LIB) L. G. Hanscom Field Bedford, Massachusetts 01730

13. ABSTRACT

This report supplements earlier attempts at modelling. Its elements are the result of a group effort, which is continuing. The arctic ionosphere and its dynamics are described as a fairly self-consistent empirical quasi-instantaneous model, adaptable to later improvements. The definitions are in analog form using tables, graphs, and analytical formulas. The model parameters controlling the arctic ionosphere are substorm time and intensity and oval number Q. Emphasis is given as to how those parameters may be obtained in near-real-time. For this purpose, two superimposed coordinate systems and two reference latitudes are introduced. The model assumes absence of sunlight; it provides rules for adding the sunlit contribution and for matching the arctic model to the moderate-latitude ionosphere.

DD FORM 1 NOV 65 1473

Unclassified
Security Classification

14. KEY WORDS	LINK A		LINK B		LINK C	
	ROLE	WT	ROLE	WT	ROLE	WT
Arctic ionosphere						
Arctic propagation						
Model ionosphere						
Real-time ionosphere						
Instantaneous ionosphere						

Abstract

This report supplements earlier attempts at modelling. Its elements are the result of a group effort, which is continuing. The arctic ionosphere and its dynamics are described as a fairly self-consistent empirical quasi-instantaneous model, adaptable to later improvements. The definitions are in analog form using tables, graphs, and analytical formulas. The model parameters controlling the arctic ionosphere are substorm time and intensity and oval number Q. Emphasis is given as to how those parameters may be obtained in near-real-time. For this purpose, two superimposed coordinate systems and two reference latitudes are introduced. The model assumes absence of sunlight; it provides rules for adding the sunlit contribution and for matching the arctic model to the moderate-latitude ionosphere.

Contents

Contents

Illustrations

Tables

Analog Model 1972 of the Arctic Ionosphere

1. INTRODUCTION

This paper supplements previous related papers (Gassmann, 1970, 1972; Buchau, 1972; Buchau and Hurwitz, 1972; Pike, 1972; Wagner, 1972). It reviews the present situation of empirical modelling and refers to results which at this time appear consistent and mature enough to serve as ingredients for modelling. Those results are then further modified and supplemented by postulations in order to arrive at a fairly self-consistent model in analog form. Although the utilized facts have been screened through a group effort (see acknowledgments) extending through several years and although two major breakthroughs were achieved by means of some thousand hours of airborne ionogram taking and by satellite observations, the resulting model still is pretentious and incomplete. Hopefully, however, it presents a structure which will not disintegrate with the emergence of new facts but rather will be able to incorporate them.

(Received for publication 1 March 1973)

2. COORDINATE SYSTEMS

2.1 CGL/CGT

This coordinate system of Corrected Geomagnetic Latitude and Corrected Geomagnetic (local) Time is the basic reference system (Whalen, 1970). We presently are using the original definition of Hakura, but mainly for consistency. The newer version due to Gustafsson (Buchau and Hurwitz, 1972) or the Invariant Latitude may be used as well, since the differences are smaller than the presently achievable model accuracies.

A fair tolerance is also allowable with respect to magnetic time. Corrected geomagnetic (local) time (CGT or CGLT) may be substituted by local magnetic time (LMT) of older definitions without resulting in significant changes in the statements of the model.

2.2 Q Latitude/CGT

This coordinate system is closely related to the CGL/CGT system; it is derived and extrapolated from the superposition of all 9 Feldstein's Auroral Ovals from Q=0 to Q=8 and is an idealized version of the individual southern borderlines. The Q latitudes are related to CGL by an equation by Starkov (1969) (which incidentally results in the simple relation: approximately one unit Q latitude = -one degree CGL). We adopted the quantity X in Starkov's equation as "Q latitude"; it is represented by concentric circles about the centerpoint at 84.9° CGL and 00.8h CGT. The equation is:

$$90^{\circ} - X = 18 + 0.9\,Q + 5.1 \cos\left(\frac{360}{24}\,Y - 12\right), \qquad (1)$$

in which X in degrees CGL is the equatorial boundary of the oval and Y = CGT in hours CGT is the geomagnetic local time. Both coordinate systems are shown in Figure 1.

3. REFERENCE LATITUDES

The model employs two reference latitudes, one for each coordinate system. Reference Latitude I refers to Q latitude; its rationale is described below. Reference Latitude II refers to CGL/CGT coordinates; it is presently used for the position of the equatorward trough wall only and is described in Section 7.4.

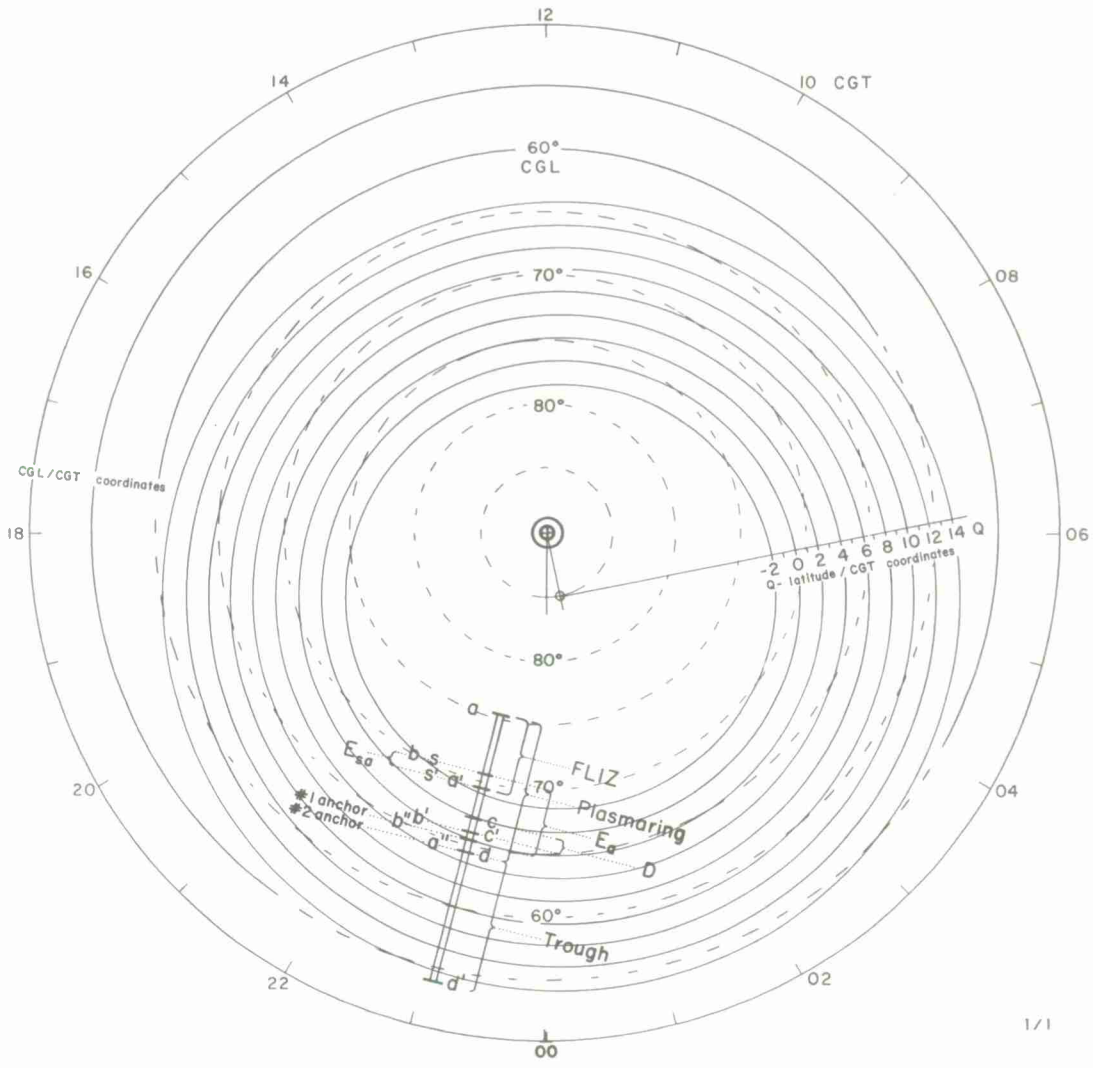

Figure 1. The Two Coordinate Systems Are Shown: Corrected Geomagnetic Latitude vs Corrected Geomagnetic (local) Time (CGL/GGT) and Q Latitude/CGT. For the local time sector of 23 CGT the latitudes and designations of the various layers are shown schematically (for approximately Q=3 prior to substorm)

3.1 Reference I Derived in Real-Time

As an alternate and more practical approach to defining the locations of the ionospheric layers as functions of geomagnetic activity, and so forth (K_p, A_p, Q, AE, solar wind) we propose to utilize Reference Latitude I. All other features of the arctic ionosphere are then anchored to this time-varying reference. Only the real-time observation of one or more anchor features is required. We propose

to define No. 1 anchor feature as the latitude where, in large scale synoptic airglow pictures such as those obtainable from satellites or from a chain of ground-stations, near magnetic midnight, the southern edge of subvisual glow appears. One analysis, which is being conducted jointly with the AWS Global Weather Centre, shows that this glow is likely identical with the auroral E layer (E_a). The No. 2 anchor feature is defined as the poleward edge of the trough as identifiable on backscatter records and which the Goose Bay ionosonde, for example, is able to see about 30 percent of the time.

Another prospective candidate for a real-time anchor feature is the southern edge of HF clutter of a northward looking radar. We have observed such clutter on backscatter records of Polar Fox II. At this time, however, it is not resolved whether the southern edge is identical to that of the E_a layer or of the plasma ring.

The procedure for establishing Reference Latitude I from the location of the anchor features is described in Section 6. It is designed such that the reference latitude does not change during a substorm while the latitude of the anchor feature does.

3.2 Reference I Derived From K_p

In the absence of real-time observations the knowledge of K_p may be used as a substitute in order to arrive at Reference Latitude I. In this case the time scale is 3 hours and all statements represent a smear over time, that is a condition averaged over substorms. The following relations, valid for the sector near midnight, exist:

$$\text{No. 1 anchor (curve b'')} \quad [\text{degrees CGL}] = 69^{\circ} - 1.0^{\circ} K_p \quad \text{(Liska and Turunen, 1970)} ; \tag{2}$$

$$\text{No. 2 anchor (curve a'')} \quad [\text{degrees CGL}] = 65.3^{\circ} - 2.3^{\circ} K_p \quad \text{(Andrews and Thomas, 1969)} . \tag{3}$$

The relation between anchor latitude and reference latitude is simplified in this case (substorm time being absent): The latitude of the reference is identical to that of No. 2 anchor and is 1° CGL smaller than that of No. 1 anchor. The conversion from CGL to Q latitude at midnight may be accomplished using Figure 1.

In the absence of real-time information another boundary may be computed from K_p, namely a' of the FLIZ (Section 7.1) (Pike, 1972):

$$\text{boundary a' [degrees CGL]} = 78.25^{\circ} - 1.2^{\circ} K_p . \tag{4}$$

However, this latitude of a' is defined for the noon-sector (12 hours CGT) only. After conversion from CGL to Q latitude at 12 CGT the boundary a' extends then along that particular Q latitude into all CGT sectors.

4. THE Q PARAMETER

This parameter is useful in defining the general (not single substorm related) condition resulting from the history of substorms during the past days. This condition determines the size of the auroral oval as it results from the state of the ring current. Instead of determining Q from magnetograms (which is impractical to do in real-time) we propose to turn the original procedure of Feldstein and Starkov (1967) around and define an instant relation between Q and the observed size of the oval. This is accomplished by postulating that our reference latitude is identical with the southern edge of the auroral oval at midnight as defined by Eq. (1). The proper value of Q follows then from Eq. (1):

$$Q = 74.4 - 1.11 \cdot \text{degrees CGL of Reference I} . \qquad (5)$$

For example, reference I = 67°, and 64° CGL results in Q = 0, and 3, respectively.

5. SUBSTORM PARAMETERS

5.1 Start of Substorm

We propose to maintain the definition of substorm time T=0 by Akasofu: a sudden brightening of a discrete arc followed by its rapid northward movement. For a more practical real-time observation of T=0, it is proposed to use the micropulsation Pi2 (sporadic magnetic fluctuations with periods between 40 and 300 seconds). This type is observable at moderate latitudes by induction coils, and from such a record a decision whether and since when a substorm has been in progress may be made within 5 minutes after T=0. Other prospective but not yet sufficiently explored means of determining T=0 are provided by satellites. One is the heliocentric satellite (planned by NASA for 1976-78, which would allow the observation of the instant of reversal of the interplanetary magnetic field from northward to southward and the duration of this abnormal field direction. Another geostationary satellite is in the planning stage and will measure protons of the energy range from 50 keV to 150 MeV. Changes in the spectrum have been indicative of the start of a substorm (Hones, 1972). Another satellite, already in

existence at about 6 earth radii, measures the sudden increase of plasma density. Those phenomena have proven correlations with the start of substorms.

5.2 Intensity of Substorm

We assume that 3 grades of substorm intensity will be distinguishable from the observations above: 1 small, 2 medium, 3 large. More precise definitions must be established later when the observational methods mentioned in Section 5.1 are better explored.

6. THE LAYER BOUNDARIES IN THE MIDNIGHT SECTOR

Figure 1 shows the scheme of the latitudinal positions of the various ionospheric features near midnight. Most of them extend in ring-like shape along one of the two coordinate systems indicated and this is specified in Section 7. The indicated positions are typical for moderate magnetic activity (Q=3) and prior to a substorm. For modelling purposes the designations a through d' of the layer latitudes apply strictly along the sector of 23 CGT. The anchor features No. 1 and No. 2 are also indicated, coinciding with the borderlines b'' and a'', respectively. Those positions will be defined below in terms of Q latitudes.

A schematic and typical vertical meridional cross section through the midnight ionosphere along 23 CGT is shown in Figure 2. In our model the borderlines a through d' float upon latitudes according to certain rules. For the midnight sector, which serves as CGT reference, those basic rules are expressed in analog form and plotted in Figure 3. This figure defines for exactly 23 CGT the latitudes

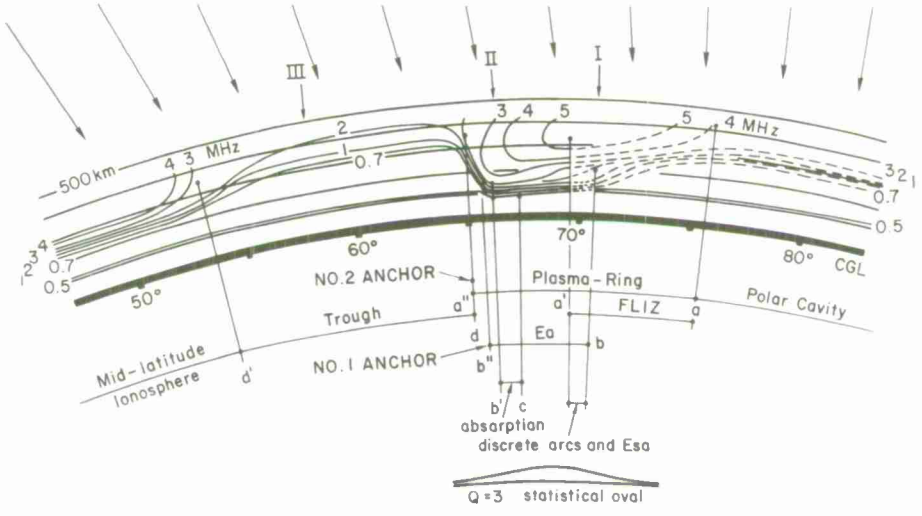

Figure 2. Vertical Meridional Cross Section Along 23 CGT. The figure shows the same scheme and designations of the ionospheric layers as in Figure 1

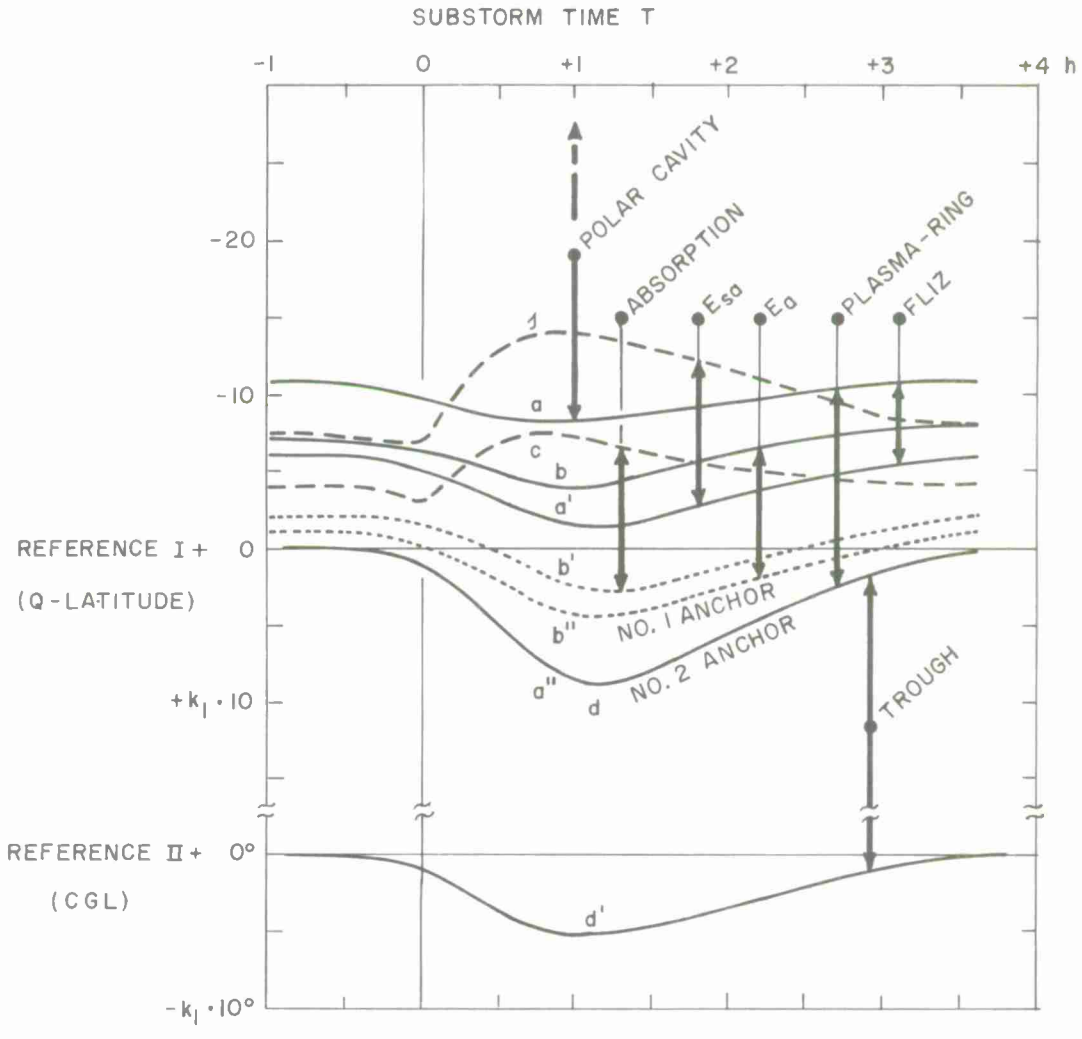

k_1	0.5	1.0	1.5
SUBSTORM INTENSITY	1	2	3

Figure 3. The Latitudinal Movements of the Various Layer Borderlines vs Substorm Time T. The plot applies for 23 CGT. The upper plot's ordinate in units Q latitude relative to Reference Latitude I. Note that only the southward ordinate (Reference I +) is normalized by the factor k_1. The lower plot's ordinate is in degrees CGL relative to Reference Latitude II, normalized by k_1. The proposed dependence of k_1 on substorm intensity is tabulated at the bottom of the figure. Solid and dotted curves are valid instantly for all CGT, according to certain rules. Dashed curve represents "surge" and provides entree into Eq. (12)

of the various borderlines vs substorm time. It is assumed that no previous substorm occurred less than 3 hours ago and that no new substorm starts before T=3 hours.

The swing of curves b', b'', a'' depends on substorm intensity. Note, the Reference I + ordinate of the upper plot is in normalized units of Q latitude relative to the Reference Latitude I. The latter is determined by observation as specified below. The normalizing factor k_1 is equal to one for a medium substorm intensity; its value is plotted in the lower corner of Figure 3. The k_1 plot is preliminary and should be improved as soon as a more precise definition of substorm intensity (Section 5.2) has emerged.

The ordinate of the lower plot (curve d') is in normalized degrees CGL relative to Reference Latitude II (Section 7.4).

Reference Latitude I is derived from the real-time observation near midnight of at least one of the anchor features. The predicted behavior of these features is indicated in Figure 3 as function of T. The actual observation near midnight of the Q latitude of each anchor feature vs time will yield a similar curve which, after knowledge of T and of substorm intensity is obtained from other sources (Section 5), can be normalized (using k_1) and matched to the corresponding curve in Figure 3. In this way the Reference Latitude I is established. This may even be possible from limited time sections of the anchor feature curves, that is when there is no continuous record available. In the absence of real-time observations the reference latitude may be derived according to Section 3.2.

7. THE LAYER DIMENSIONS ALONG THE ENTIRE AURORAL OVAL

In the model proposed at this time the layer boundaries, as defined for 23:00 CGT in Figure 3 at any substorm time T, extend into other CGT sectors according to the following rules.

7.1 The FLIZ and Plasma Ring

We call the ring-like F layer between a and a'' the plasma ring and the part of it between a and a' the FLIZ (F layer irregularity zone). The boundaries a, a', and a'' (solid lines in Figure 3) apply instantly to all CGT sectors along constant Q latitudes.

The plasma frequencies quoted in the following refer to magnetic conditions Q=3; accordingly the values are normalized by attaching to them the factor k_2. Table 1 contains the proposed dependence of k_2 on Q.

Table 1. Proposed Dependency of k_2 on Q

k_2	0.5	0.7	0.9	1.0	1.2	1.4	1.5		
Q	0	1	2	3	4	5	6	7	8

In the center of a to a'', approximately at the latitude of a', the value of f_oF is $k_2 \cdot (5 \pm 1)$ MHz. The layer maximum occurs at a height of h'F = 310 ± 25 km. The half thickness from layer maximum to bottom is 140 ± 20 km. Above the height of the layer maximum the electron density may be modelled as a Chapman layer.

The values near latitude a are $f_oF = k_2 \cdot (3 \pm 1)$ MHz and $h_{max}F = 350 \pm 50$ km respectively, with half thickness of 80 ± 15 km. The corresponding values at latitude a'' are $k_2 \cdot (3 \pm 1)$ MHz and 250 ± 25 km, respectively, with half thickness of 100 ± 20 km. All these values apply to all UT's.

There is UT dependence with a minimum in plasma frequencies at 06 UT. Although this UT dependence, which is modelled in Gassmann (1970), is indeed real, its effect relative to the other remaining uncertainties is minor and is being disregarded at this time.

The FLIZ is that part of the plasma ring the contour lines of which are heavily modulated in an irregular manner (Figure 2) causing HF scatter.

North of latitude a appears a region, sometimes called the polar cavity, which has less scattering characteristics but larger temporal and/or spatial variations of not identified correlation. Vertical soundings show coarse irregularities of dimensions of tens of km. However, in oblique illumination (angle of incidence against vertical larger than 70^o) the polar cavity ionosphere may be regarded as a smooth layer with $f_oF = 3 \pm 2$ MHz and $h_{max}F = 380$ km, with a half thickness of 100 km. The ionosphere in the polar cap (from 75^o to 90^o CGL) is very variable and the least explored.

At latitude a'', which we assume is identical to d (the poleward trough wall), there is at heights above 300 km a steep horizontal gradient of the plasma frequencies of:

$$\frac{(Q+4)^2}{23} \ [\text{MHz}/1^o \text{ CGL}] \ , \qquad (6)$$

which for Q = 3, for example, amounts to 2.1 MHz per 1^o CGL.

Approximate characteristic vertical height profiles for three latitudes I, II, and III marked in Figure 2 are plotted in Figure 4.

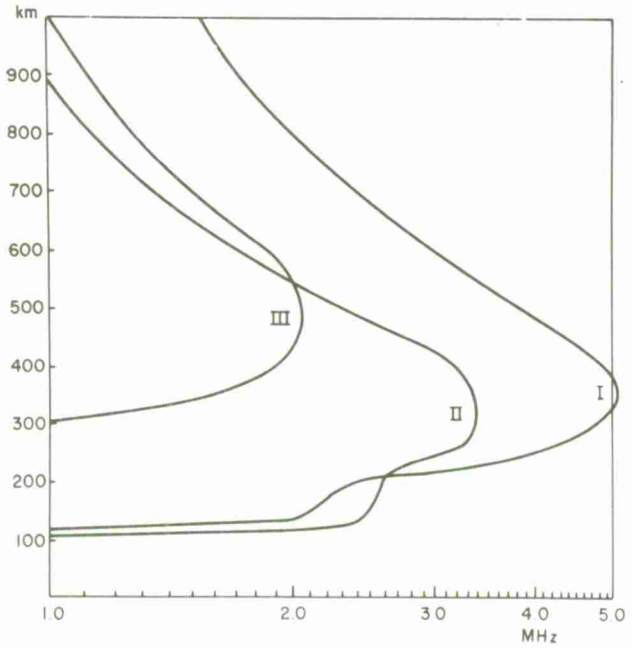

Figure 4. Characteristic Height Profiles at Points I, II, and III Marked in Figure 2

7.2 The Auroral E Layer (E_a)

The northern boundary b applies instantly to all local CGT sectors along constant Q latitude. The southern boundary b'' as well as the location of b' of maximum f_oE_a (dotted lines) apply also instantly for all time sectors; however, they follow along constant Q latitude in the night sectors only; from 06 CGT eastward the boundaries b' and b'' follow along constant CGL through the day sectors until they meet the original Q latitudes near 18 CGT. This rule places the southern edge of the E_a layer in the midday-sector south of the F layer, in accordance with the airborne observations, while in the midnight sector the E_a layer is embedded in the plasma ring.

The value f_oE_a(max) at b' is plotted in Figure 5 as a function of Q. At points b and b'', f_oE_a is 0.6 times the value plotted in Figure 5. The horizontal gradient of the plasma frequencies at 120-km height at the latitude of b'' also follows formula (6). This results in very steep contour lines similar to those in Figure 2. The values of the layer bottom height are related to f_oE_a as plotted in Figure 5, in which $h'E_a$ corresponds to the layer bottom. We have very little information on the layer's thickness; a layer half thickness of 50 km from its lower level to its maximum and of 100 km above its maximum is suggested.

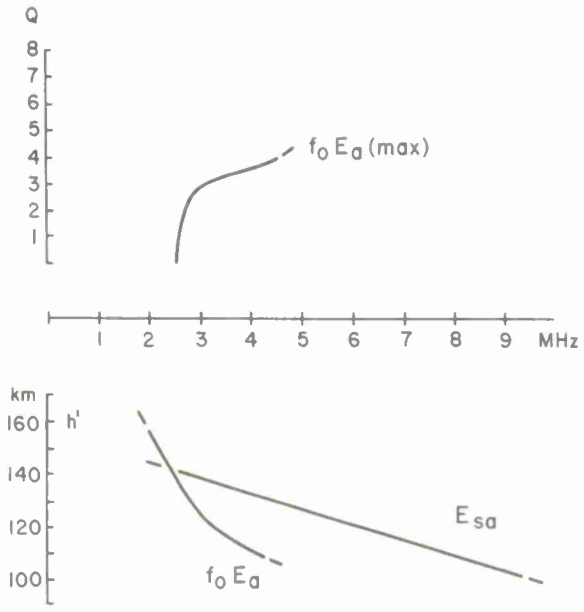

Figure 5. Upper Portion: The Dependency of f_0E_a at Latitude b', Where the Value Maximizes, on Q. Lower Portion: The dependency of the height h' of the bottom of the E_a layer and of the (thin) E_{sa} layer on f_0E_a and fE_{sa}, respectively

7.3 E_{sa} (auroral sporadic E) and Discrete Arcs

(1) Prior to a substorm E_{sa} and visible discrete auroral arcs occur between b and a'. During a substorm a new poleward boundary s splits off b (Figure 3).

(2) The boundary s represents the "surge" emerging from the origin (23 CGT assumed) of a substorm. We allow this poleward movement to travel eastward and westward with a speed of 1 km/sec along constant Q latitudes, however with diminishing effect vs elapsed time (dying out) according to the following derivation:

The approximate longitudinal speed eastward and westward around the auroral oval at 1 km/sec is:

$$8\,[h\,\Delta\,CGT/h]\ . \tag{7}$$

The longitudinal difference Δ, in units of CGT, counted from substorm origin (23 CGT) toward the longitude Y [CGT] is:

$$\Delta\ CGT = \begin{cases} Y + 1 & \text{eastward}\ , \quad (8) \\ 23 - Y & \text{westward}\ . \quad (9) \end{cases}$$

The corresponding elapsed time of propagation at longitude Y is

$$\Delta \text{ CGT}/8 \text{ [h]} \quad . \tag{10}$$

We let the latitude difference between lines s and b in Figure 3 diminish to 1/e after travel along 8 hours in CGT coordinates (which corresponds to about 1 hour of elapsed time):

$$(s-b) \cdot e^{-\left(\frac{\Delta CGT}{8}\right)^2} \quad . \tag{11}$$

At any longitude Y [hours CGT] and at any selected substorm time T_x the location of borderline s is then computed from the Q-latitude values in Figure 3:

$$s = \underset{\text{at } T=T_x}{\uparrow} b + \underset{\text{at } T=T_x - \frac{\Delta CGT}{8}}{\uparrow} (s-b) \cdot e^{-\left(\frac{\Delta CGT}{8}\right)^2} \quad . \tag{12}$$

(3) Both auroral sporadic E (E_{sa}) and discrete auroral arcs occur between s and a' (see Figure 3). In this specified latitude range the probability of occurrence is 80 percent of the time. The proposed normalized value of fE_{sa} is:

$$\text{for } T < 0, \quad fE_{sa} = k_2 \cdot (4 \pm 1) \quad \text{MHz} ,$$

$$\text{for } T > 0, \quad fE_{sa} = \left(1 + \frac{k_1}{1.5} \cdot e^{-T}\right) \cdot k_2 \cdot (4 \pm 1) \text{ MHz} . \tag{13}$$

Thus, at T=0 a sudden enhancement occurs and this formulation incorporates a decay within 1 hour after T=0. The height of this thin layer depends on fE_{sa} and is plotted in Figure 5.

The relatively small band between s and a' expands during a substorm and extends according to the above rule. The average over many substorms produces the statistical picture of E_{sa} as it appears in Gassmann et al (1972, page 23). We propose at this time to disregard the relatively small variations which are known to exist during changes of season, sunspot cycle, and UT.

7.1 The Subauroral Trough

This F-layer feature extends from d to d'. Latitude d is identical to a'' (described in Section 7.1) and represents the poleward trough wall. As to the latitude d' of the equatorward trough wall we have not sufficient information to

establish a correlation with Q, K_p, substorm-intensity, and so forth. We propose at this time to introduce Reference Latitude II and to assume the position of d' according to Figure 3, in which the CGL value of d' is plotted against substorm time. The CGL value of Reference II, in turn, is derived from Carpenter's (1967) formula for the plasmapause (the latter very likely closely related to the mechanisms which cause the trough):

$$\cos^2 (\text{Reference II [CGL]}) = \frac{1}{6.(1-Q/10)} , \tag{14}$$

in which Q represents the maximum Q value in the preceding 12 hours.
The value of f_oF in the trough varies from day to day between 0.8 and 6 MHz. The trough is probably caused by the loss of ionization due to cross-field diffusion which in turn is likely to vary with magnetic activity. We conceive the value of f_oF in the trough as a Q-dependent fraction of the value predictable for 60^o CGL (60^o geographic latitude may be substituted) from extrapolation of the moderate latitude ionosphere. Accordingly we define the model value below and propose to assume this value as being constant across the trough and only dependent on UT:

$$f_oF\ (UT)_{\text{trough}} = \frac{2}{2+Q} \cdot f_oF\ (UT)_{60^o \text{ lat.}} \pm 1\ [\text{MHz}] . \tag{15}$$

The height of the layer maximum may be taken as $h_{max} = 470 \pm 50$ km with a half thickness of 150 ± 30 km. A characteristic height profile is shown in Figure 4, Curve III.

7.5 HF Absorption

The ionospheric D layer is not included here. Our own data base, however limited, appears contradictory so far; we have seen many occasions when there was no absorption, even during large substorms overhead, in areas where high absorption should occur according to published statistics. The best information has been created by the Hultquist Working Group on Substorms (Berkey et al, 1971) and those results have been formulated into a model by Elkins (1972). This model however is statistical in nature and does not employ the concept of anchor latitudes to be observed in real-time.

In order to facilitate incorporating future results on absorption and merging of models we have indicated in Figures 1, 2, and 3 the latitudes c and b'. Those might approximately define the northern and southern boundaries, respectively, of absorption near midnight. Propagation of these borderlines toward the east along constant CGL with a certain speed and decay may then be formulated similarly as formulated above for E_{sa}.

8. THE EFFECT OF SOLAR ILLUMINATION

All ionospheric layers described here are abstractions, valid for the arctic night, that is assuming no illumination by the sun. In reality parts or all of the Arctic might be illuminated depending on season and this requires computing an ionosphere which results from two contributions. The first is due to precipitation of electrons and protons and takes place in the two arctic coordinate systems described. The second is due to electromagnetic solar radiation and is usually described in the geographical coordinate system. The problem of the required various conversions among these coordinate systems has been treated by Buchau and Hurwitz (1972). The other problem is how to add the two contributions. The following rules are suggested: For the E layer the squares of the electron densities, whereas in the F layer (above 250 km) the sums of the electron densities are added together. More details and discussion are in Gassmann (1970).

9. THE MATCHING OF THE ARCTIC AND MODERATE LATITUDE MODELS

It is important for computerized ray tracings that at the borderline where the models of the arctic and moderate latitude ionosphere join no artificial discontinuities appear. The arctic ionosphere model presented here extends down to latitudes of the equatorward trough wall d'. We propose to use this natural discontinuity as a convenient means of matching. At any fixed UT there belongs to any point along borderline d' in (CGL/CGT) a particular geographical location. We propose assuming a ramp along d' with an inclination against the horizontal of 25° along the magnetic meridian by which the plasma-frequency height levels as defined in the trough (according to Section 6.4) are being connected to the corresponding height levels at moderate latitudes, such as modelled by Damon et al (1970) and supplemented by Cookingham (1972) and Rush (1972).

10. CONCLUSIONS

In order to facilitate check-ups on the usefulness of this model a computation sheet has been provided (Table 2) which pertains to Eqs. (11) and (12) and to Figure 3. As an illustration of how arctic ionospheres would appear as the result of the graphs, equations, and rules of this particular 1972 model, two cases are chosen. The results are plotted in Figures 6 and 7. For Reference I the Q latitude of 3 is assumed. Figure 6 shows the borderlines of the various layers for a time prior to the start of a substorm. The corresponding view in the vertical plane

Table 2. Computation Sheet for Position s (poleward boundary of E_{sa} and discrete arcs)

Selected Substorm Time T = T_x = ... h ; k_1 = ... (from estim. intensity + Figure 3)								
1	2	3	4	5	6	7	8	9
Longitude Y [h CGT]	Δ CGT	$\frac{\Delta \text{ CGT}}{8}$	$e^{-\left(\frac{\Delta \text{ CGT}}{8}\right)^2}$	T= T_x minus Column 3 [h]	(s - b) fr. Fig. 3 at T=Column 5	Eq. (11) Columns 4×6	b fr. Fig. 3 at T=T_x	Eq. (12) s=Cols. 7+8 [Q Latitude]
							Reference 1 plus	Reference 1 plus
23	0	0.00	1.00					
00	1	0.13	0.99					
1	2	0.25	0.94					
2	3	0.38	0.87					
3	4	0.50	0.78					
4	5	0.63	0.68					
5	6	0.75	0.57					
6	7	0.88	0.46					
7	8	1.00	0.37					
8	9	1.12	0.28					
9	10	1.25	0.21					
10	11	1.38	0.15					
11	12	1.50	0.10					
12	11	1.38	0.15					
13	10	1.25	0.21					
14	9	1.12	0.28					
15	8	1.00	0.37					
16	7	0.88	0.46					
17	6	0.75	0.57					
18	5	0.63	0.68					
19	4	0.50	0.78					
20	3	0.38	0.87					
21	2	0.25	0.94					
22	1	0.13	0.99					
23	0	0.00	1.00					

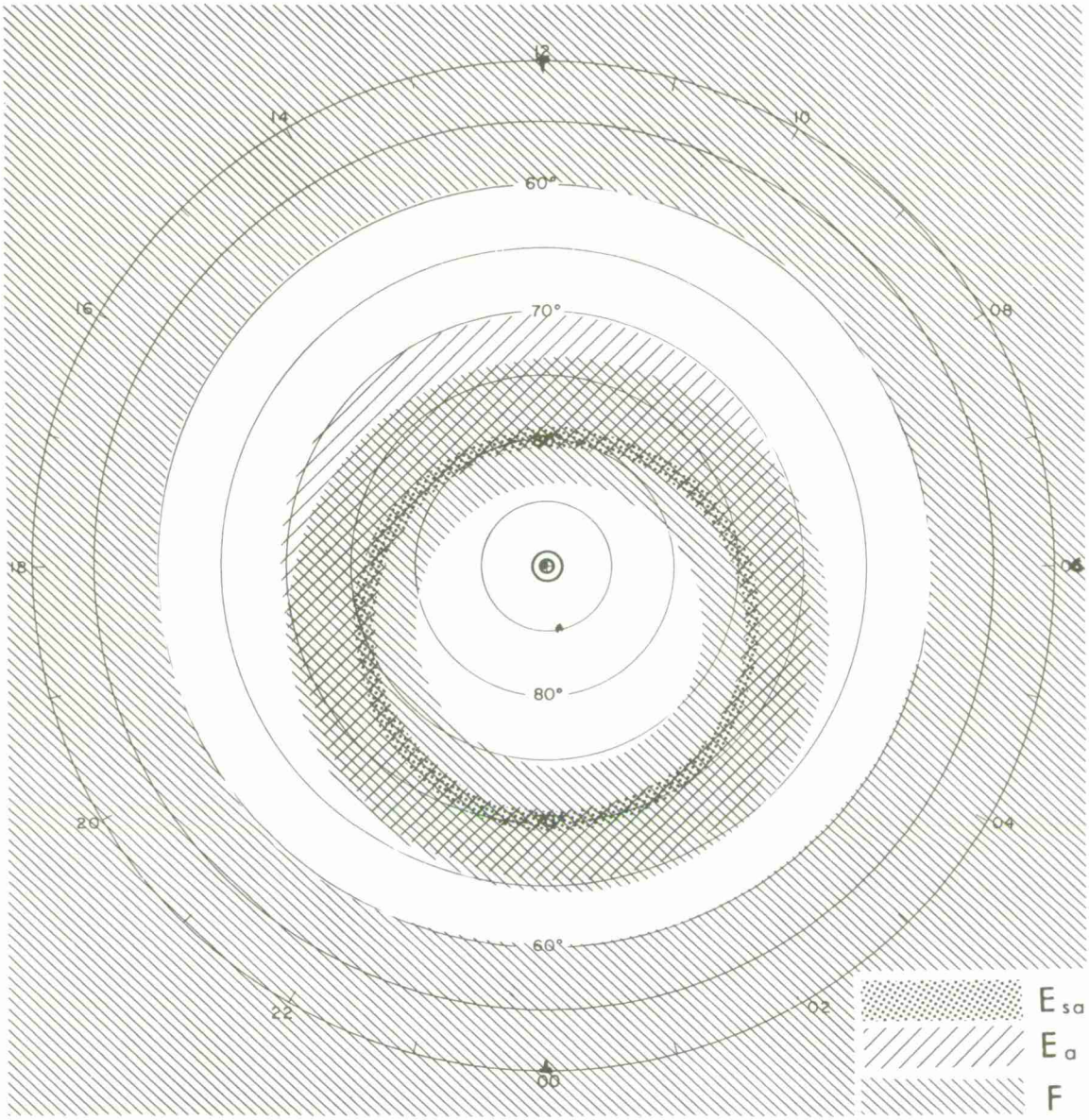

Figure 6. Example of Instantaneous Model Ionosphere in Geomagnetic Coordinates for a Time Prior to Start of a Substorm.
Assumed Reference I (to be observed in real-time): +3 Q Latitude.
Assumed Reference II (to be derived in real-time): 60^{o} CGL

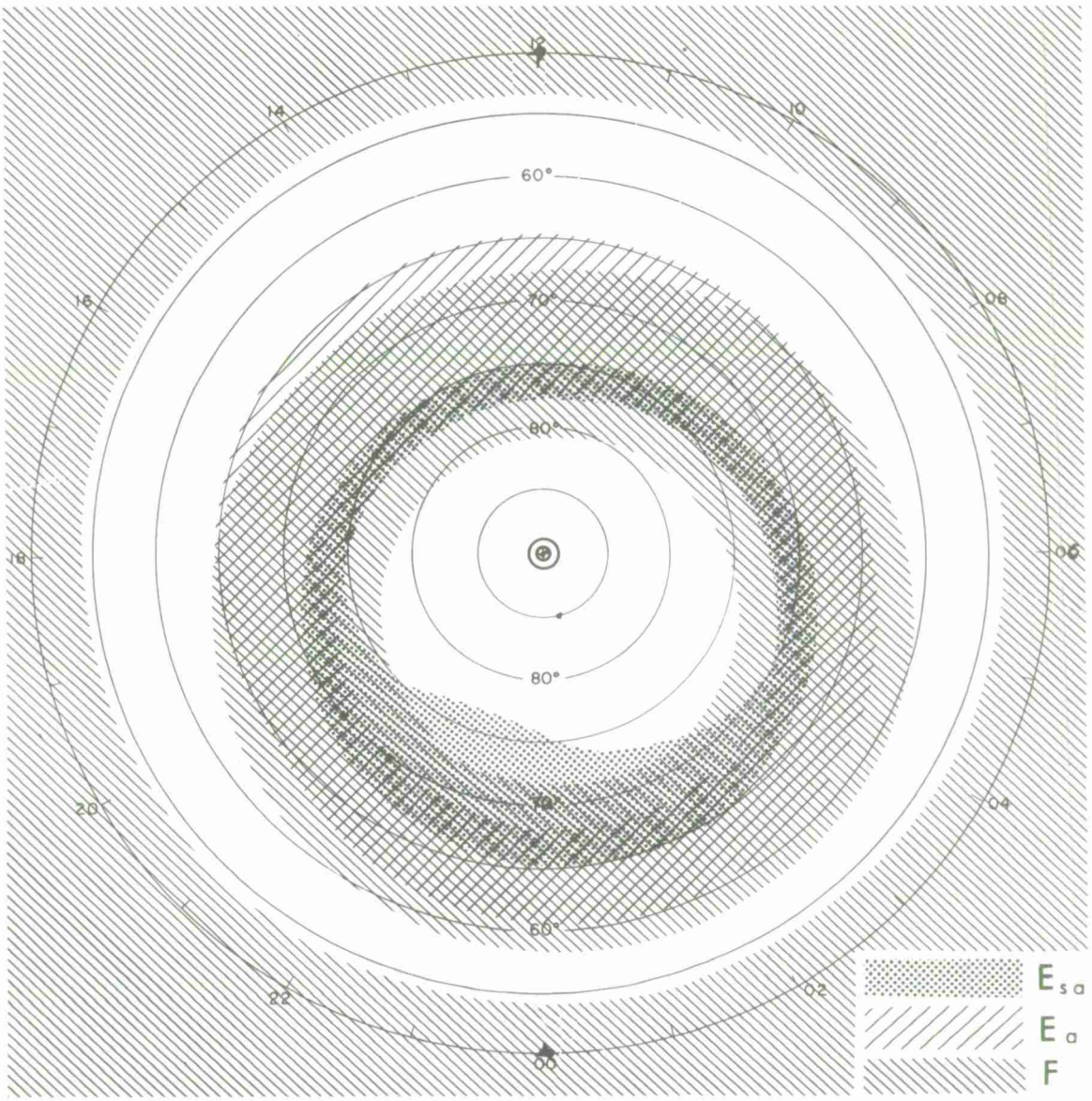

Figure 7. Example of Instantaneous Model Ionosphere in Geomagnetic Coordinates for Substorm Time $T=T_X$ = 0.8 h.
Assumed Reference I (to be observed in real-time): +3 Q Latitude.
Assumed Reference II (to be derived in real-time): 60^o CGL.
Assumed Substorm Intensity (to be derived in real-time): 2; $k_1=1$

along 23 CGT longitude is shown in Figure 2. Figure 7 shows the borderlines at substorm time $T=T_x = 0.8$ hours, and assumes a substorm intensity 2.

The implementation of the model, presented here in analog form, into a tool for operational use will require computerization. In the course of such a process it is likely that gaps, omissions, and contradictions appear. Nevertheless, the model is designed to be able to incorporate anticipated supplements, corrections and improvements.

Acknowledgments

The various facts, concepts, and formulations used are the result of a group effort at the Boundary Interactions Branch at AFCRL with the following physicists contributing: C. P. Pike, R. A. Wagner, J. Buchau, J. A. Whalen. We had the benefit of stimulating discussions with S. I. Akasofu, L. Snyder, W. Heikkila, J. Winningham, and G. Stanley.

References

Andrews, M.K. and Thomas, J.O. (1969) Electron density distribution above the winter pole, Nature 221:223.

Berkey, F.T., Driatsky, V.M., Henriksen, K., Jelly, D.H., Shchuka, T.I., Theander, A. and Yliniemi, J. (1971) Temporal development of the geographical distribution of auroral absorption for 30 substorm events in each of IQSY (1965-65) and IASY (1969), World Data Center-A Report UAG-16.

Buchau, J. (1972) Instantaneous versus averaged ionosphere, Chap. 1 in AFCRL-72-0305.

Buchau, J. and Hurwitz, M.G. (1972) Coordinate conversion and other computer programs, Chap. 5 in AFCRL-72-0305.

Carpenter, D.L. (1967) Relations between the dawn minimum in the equatorial radius of the plasmapause and Dst, K_p, and local K at Byrd Station, J. Geophys. Res. 72(11):2969-2971.

Cookingham, R.E. (1972) Modelling the Bottomside Electron Density Profile, AFCRL-72-0340.

Damon, T.D. and Hartranft, F.R. (1970) Ionospheric Electron Density Profile Model, Technical Memorandum 70-3, 4th Weather Wing (MAC), Ent AFB, Colorado 80912.

Elkins, T.J. (1972) A Model of Auroral Substorm Absorption, AFCRL-72-0413.

Feldstein, Y.I., and Starkov, G.V. (1967) Dynamics of auroral belt and polar geomagnetic disturbances, Planet. Space Sci. 15:209-229.

Gassmann, G.J. (1970) An Ionospheric Model for the Arctic, AFCRL-70-0562.

Gassmann, G.J. (1972) On modelling the arctic ionosphere, in Radar Propagation in the Arctic, AGARD-CP-97, pp. 2-1 to 2-8.

Gassmann, G.J. (1972) Model of arctic sporadic E, Chap. 3 in AFCRL-72-0305.

Hones, E. (1972) Los Alamos Scientific Laboratory, private communication.

Lizka, L., and Turunen, T. (1970) On the relation between the auroral particle precipitation and the ionospheric trough, Kiruna Geophys. Obs. Preprint 70:315.

Pike, C.P. (1972) Modelling the arctic F-layer, Chap. 4 in AFCRL-72-0305.

Pike, C.P. (1972) Equatorward shift of the polar F-layer irregularity zone as a function of K_p index, J. Geophys. Res. 77(34):6911-1915.

Rush, C.M. (1972) Improvements in Ionospheric Forecasting Capability, AFCRL-72-0138.

Starkov, G.V. (1969) Analytical representation of the equatorial boundary of the oval auroral zone; translation in Geomagn. a. Aeronomy 9(4):614.

Wagner, R.A. (1972) Modelling the auroral E-layer, Chap. 2 in AFCRL-72-0305.

Whalen, J.A. (1970) Auroral Oval Plotter and Nomograph for Determining Corrected Geomagnetic Local Time, Latitude, and Longitude, AFCRL-70-0422.